IET Smart Grid

Research Article

IET Journals
The Institution of Engineering and Technology

Realisation of RPS from electrical home appliances in a smart home energy management system

eISSN 2515-2947
Received on 5th March 2019
Revised 24th August 2019
Accepted on 5th September 2019
E-First on 7th October 2019
doi: 10.1049/iet-stg.2019.0066
www.ietdl.org

Samir Gautam[1] ✉, Dylan Dah-Chuan Lu[2], Weidong Xiao[1], Yuezhu Lu[1]

[1]*School of Electrical and Information Engineering, The University of Sydney, New South Wales, 2006, Australia*
[2]*School of Electrical and Data Engineering, The University of Technology Sydney, New South Wales, 2007, Australia*
✉ *E-mail: samir.gautam@sydney.edu.au*

Abstract: With the increasing integration of photovoltaic power generation in the low-voltage distribution network, the grid voltage regulation becomes critical, which demands support from different resources. This study presents the feasibility study of home appliance to be applied for appliance to grid mode of operation. The analysis includes the amendments in topology and control to support the concept of supportive platform provided by smart home and smart grid. Home appliances are then proposed as new distributed reactive sources, which are utilised to resolve the issue of voltage regulation, as well as produce reactive power locally for voltage stability. This study discusses the technical transitions in current home appliance to accommodate auxiliary functionality of grid reactive power support (RPS) and how it can fit in the home energy management system architecture to provide the required RPS.

1 Introduction

The increase in renewable power generation, especially the installation of photovoltaic (PV) systems in residential area, is introducing concerns regarding grid voltage quality at distribution level. The major one being the voltage rise and voltage fluctuations due to excessive power export from PV to grid and intermittent nature of PV sources [1–3]. This can be serious at daytime when the real power consumption is lower compared with high injection of active power to grid from PV inverters, thereby causing reverse power flow and overvoltage [4]. Correspondingly, the requirement of grid support at low-voltage distribution level is expected to increase [3].

Conventional approaches of grid support such as on load tap changer, voltage regulators, manually switched capacitor banks, static compensator and volt-ampere reactive (VAR) regulators are somewhat ineffective for voltage regulation from either their installed location, high operating cost, discrete reactive power output or response time to reactive support [5, 6]. Another approach of updating distribution grid by increasing conductor size to reduce resistance of low-voltage lines is going to be a costly affair [7]. Employing PV inverters themselves for reactive power exchange has possibly been the most attractive solution for voltage regulation in low-voltage distribution system [8, 9]. Furthermore, this also results in scattered reactive resources in power system and at the point, where they are highly desired. Turitsyn *et al.* [10] have highlighted the benefits of distributed reactive power support (RPS) in terms of efficiency, flexibility, stability and reliability. Ghasemi and Parniani; Tonkoski *et al.*; and Ghosh *et al.* [11–13] mention how the overvoltage issue at the distribution network, especially at feeder end, limits the instalment of PV system capacity. They have proposed using the latent capacity of inverter to regulate voltage by either supplying or absorbing reactive power. If this approach cannot offer required voltage profile, then active power curtailment (APC) of the PV system is suggested. Throttling of the active power injection from the PV units into the grid becomes unfavourable to PV system owners. At the times of high irradiance, the reactive power capability of the PV system decreases and applying real power curtailment could cause the energy wastage, which could have been otherwise sent to remote location for usage and storage.

The PV inverter alone cannot cater to the required VAR without increasing its apparent power rating, considering the time of peak PV generation (real power) limits the VAR capability. The idea of using plug-in electric vehicle (EV) for providing vehicle to grid support functionality is already a topic of ongoing research. This has been realised using onboard bidirectional charger capable of exchanging reactive power with grid at the point of charging location [14]. However, the location of the EV cannot be precisely confirmed and at daytime tends to be away from residential areas. Research shows the overvoltage to occur, especially at daytime due to unbalance between high PV generation and low load demands [15]. Having additional sources of reactive power dispersed in the distribution network is always beneficial for neutralising the voltage rise problem. Moreover, through this, the PV hosting capacity (ability of grid to allow connection of additional PV systems) of the distribution network can also be boosted without increasing the voltage and compromising on PV system active power output [16].

Modern home appliances comprise of power electronics for efficient utilisation and power conversion, and extensively distributed. The home appliances generally take part in grid support by controlling its active power consumption known as demand-side management [17], where the operating times of the appliances are altered directly or indirectly to change the power profile of network and consequently influence voltage regulation. However, utilising them for RPS to the grid is new, but opens up more opportunities to microgrid control and management. Fig. 1 illustrates a survey of the usage pattern of appliances in a single home over 1 week [Source: Pecan Street Inc. Dataport 2017.]. It shows that the appliances were used randomly for small proportion of daily time and there are large periods of inactivity. The stationary nature, spare power processing capacity and extensive distribution are motivating factor to use appliances for ancillary function of RPS at underutilised and idle times [6]. These can aid in regulating voltage profile, power factor improvement and reactive power supply.

Predominantly, most of home appliances power supplies consist of a diode bridge followed by power factor correction (PFC) circuit, generally a boost converter [18–21]. A DC-link (DCL) capacitor filter separates AC–DC rectification with subsequent power processing stage. These power supplies are primarily designed for unity power factor operation and low AC distortion. The reactive support capability is low and limited, which is discussed in [6, 22]. Hence, to fully extract benefits of the second objective, it necessitates topological modification owing to

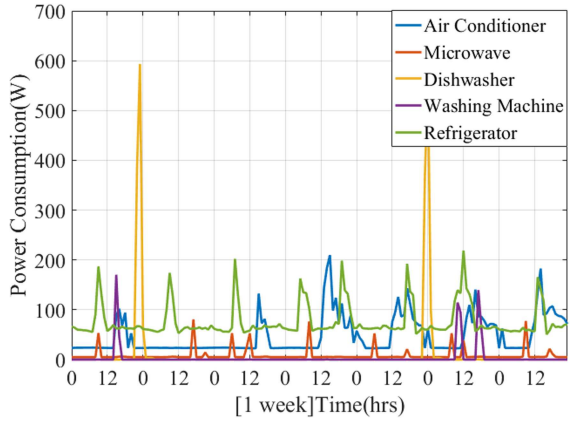

Fig. 1 *Appliance utilisation pattern in a single home in 1 week*

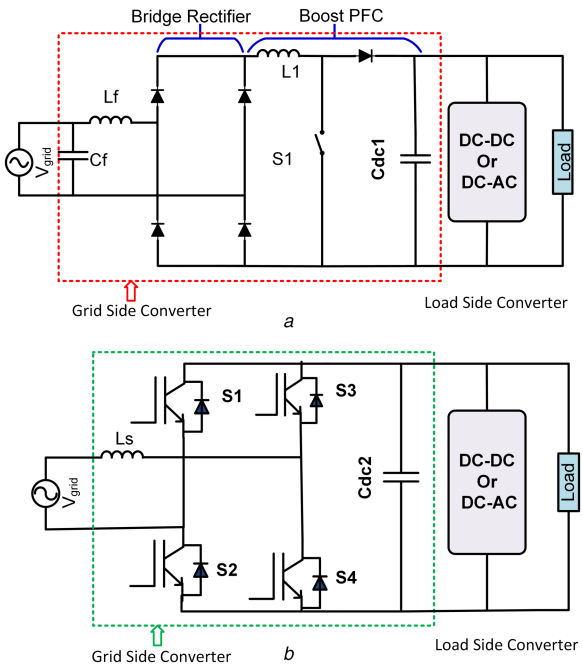

Fig. 2 *Proposed modification on the home appliance's power supply*
(a) Conventional power supply topology, ***(b)*** Power supply based on the full-bridge converter

Table 1 Home appliances and their LSCs

Appliance	Load requirement	LSC
television	various DC voltage level (low *V*, high *I*)	DC–DC [26]
WM, A/C, DW	three-phase variable *v*, *f*	three-phase DC–AC [27]
IH	single-phase high-frequency AC	single-phase DC–AC [28, 29]
microwave	high DC voltage and high AC	DC–DC [30, 31]

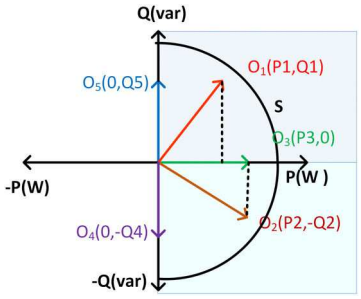

Fig. 3 *Possible operation region of the home appliance*

bidirectional power flow requirement [6]. The replacement of diode bridge rectifier (DBR) and PFC circuits, with a full-bridge pulse-width modulation (PWM) rectifier results in a generalised power supply structure as a cascaded two-stage converter. The configuration can allow bidirectional power flow and provide dynamic nature of reactive power source. Two operation modes can be realised: the regular operation mode from grid to appliance, whereas in the other additional mode appliance to grid (A2G) only RPS is performed. The evolution of smart grid [23], smart homes consisting of home energy management system (HEMS) [24] and smart home appliances [25] will make control and monitoring of these home appliances much easier.

Gautam *et al.* [6] explored the potential capability of home appliance's power supplies and provided a general framework for the realisation of grid support from it. However, the influence of additional operation mode on the system components and variables were not considered. This paper further substantiates the utilisation of the home appliance as a new distributed reactive power source available in residential area. The major changes in topology, design of components and control structure for the proposed A2G support are presented in detail. The focus is the technical transition from current home appliance to updated home appliance and how it can fit in the HEMS architecture to provide the required RPS.

The structure of this paper is as follows: Section 2 discusses the design changes in the proposed topology and control. Section 3 introduces the proposed architecture of the smart home with RPS from home appliances. Section 4 presents the simulation results of home server with appliances for A2G operation. In Section 5, cost–benefit analysis of the proposed reactive control approach is discussed. Finally, Section 6 discusses the further development regarding the proposed implementation and Section 7 summarises the concluding remarks.

2 Effect of RPS on the bridgeless power supply

A typical home appliance follows the cascaded structure shown in Fig. 2*a*. The grid-side converter (GSC) performs single-phase AC–DC conversion and is generally composed of DBR. A PFC circuit is included to meet the current harmonic standard such as IEEE 519 and IEC 61000-3-2 for input current drawn by the power supplies [21]. The load-side converter (LSC) can be either a DC–DC or DC–AC converter (single phase or three phase) depending on the load specification. Table 1 lists the load requirement and corresponding LSCs for some typical home appliances. Resonant inverters with output operating frequency at around 20–30 kHz are used for induction heating application. In washing machine (WM), induction motors and brushless DC motors are preferred due to their efficiency. Three-phase motors are replacing single-phase motors owing to efficiency, cost and performance. The inverter for the WM application will output variable frequency and voltage to attain the required wide speed of the drum for wash/spin cycle at different loads. Generally, wash cycle requires lower speed and spin cycle requires higher speed. Despite the differences in the LSCs of different types of appliances, they are generally equipped with the same GSC for AC–DC conversion and PFC circuit.

In the proposed solution, the DBR and PFC altogether are changed to a full-bridge converter to construct the GSC, as shown in Fig. 2*b*. The proposed solution is expected to provide the reduced component count, higher efficiency, better power quality performance (lower total harmonic distortion) and more controllability. The topology of the GSC is now capable of operating in two quadrants with three possible operation modes. The possible operating region is defined as (P_{load}, 0), (0, Q_{supp}) and (P_{load}, Q_{supp}) as shown in Fig. 3. Active power flow is unidirectional while reactive power can either be inductive (+ve) or capacitive (−ve) depending on the operation requirement. The RPS from the home appliance can now assist in voltage regulation of the distribution system. A typical reactive power compensation trajectory is shown in Fig. 4. When the grid voltage rises above V_{nh} or drops below V_{nl}, then appropriate reactive power can be consumed or injected into the grid to bring the grid voltage within its nominal bound. Moreover, the electricity consumers reactive

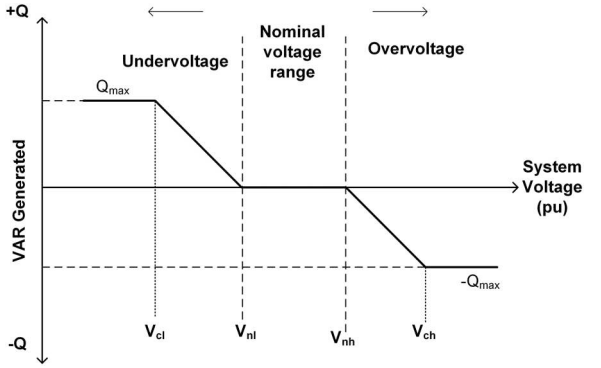

Fig. 4 *Standard reactive power control method for voltage regulation*

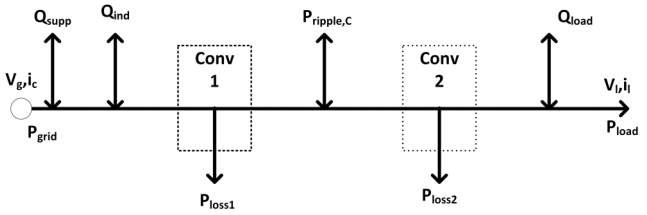

Fig. 5 *Active and reactive power flows between different stages*

power demand can also be met locally improving their power factor (closer to unity).

With the incorporation of new operation modes, the DCL capacitor that connects the GSC and the LSC shows the most impact of RPS. It acts as a reactive buffer and the modulation and control of the bidirectional AC–DC converter help to either consume or output the reactive power. In the following sections, the changes in the design of power supply components and the updated control structure are evaluated to realise the RPS from the proposed solution.

2.1 Impact on DCL capacitor and voltage

The DCL capacitor helps in maintaining the DC voltage and enables both the GSC and the load converter to work independently of each other. One of the major tasks of the DCL capacitor is to balance the instantaneous power variation between source and load. This results in capacitor voltage ripples at double of mains frequency, which though undesired is unavoidable [32]. The ripple amplitude is expected to be higher when the RPS is introduced. The selection of the DCL capacitor must consider the extra energy storage and capacitor current to accommodate the increased ripple. Also, the power transfer between DCL and load influences the DCL capacitor, which is dependent on the type of load converter used. To determine the relation between capacitance, reactive support, voltage fluctuation and load power consider the power flow graph from grid to load as shown in Fig. 5. Also, the following assumptions have been made:

- The losses in two converter stages P_{loss1} and P_{loss2} are considered low and neglected for analysis.
- The high-frequency components originating due to switching action is neglected.
- The interface inductor and DCL capacitor are assumed ideal; hence, no active power loss occurs in them.

Power ripple in the capacitor due to power transfer from the grid side occurs for all three types of LSCs. Additionally, the power flow to the load also causes ripple in the DCL capacitor if the cascaded converter is single-phase DC–AC.

Consider the phase θ_g between the grid voltage and current of frequency ω_g which is given by

$$v_g(t) = V_g \sin(\omega_g t) \tag{1}$$

$$i_c(t) = I_C \sin(\omega_g t - \theta_g) \tag{2}$$

Instantaneous input power drawn from the grid is given as

$$\begin{aligned} p_g(t) &= v_g(t) \times i_c(t) \\ &= V_g \sin(\omega_g t) \times I_c \sin(\omega_g t - \theta_g) \end{aligned} \tag{3}$$

Instantaneous power of the coupling inductor is

$$\begin{aligned} p_{\text{ind}}(t) &= v_{\text{ind}}(t) \times i_c(t) = L i_c(t) \frac{\mathrm{d}i_c(t)}{\mathrm{d}t} \\ &= \frac{\omega_g L_c I_C^2 \sin(2\omega_g t - 2\theta_g)}{2} \end{aligned} \tag{4}$$

The instantaneous power fed to the GSC is given as

$$\begin{aligned} p_{\text{conv}}(t) &= p_g(t) - p_{\text{ind}}(t) \\ &= \frac{V_g I_c \cos\theta_g}{2} - \frac{V_g I_c \cos(2\omega_g t - \theta_g)}{2} \\ &\quad - \frac{\omega_g L_c I_C^2 \sin(2\omega_g t - 2\theta_g)}{2} \end{aligned} \tag{5}$$

Similarly, the power consumed by the load is

$$p_l(t) = v_l(t) i_l(t) \tag{6}$$

The nature of load power relies on load and the type of cascaded converter present. For loads driven by DC–DC and three-phase DC–AC converters, there will be no impact on the DCL capacitor due to active power transfer toward the load side. Also, the reactive power flow between DCL and three-phase loads will have no impact on the DCL capacitor. Although each phase has the second-order harmonic sinusoidal component, the total instantaneous power is constant for the input of three-phase inverter, behaving such as a DC–DC converter. However, when single-phase inverter is used as the LSC, the impact on the DCL capacitor has to be taken into account due to the presence of the ripples at twice the load frequency. If the load frequency is ω_l, and corresponding load voltage and current have a phase difference of θ_l, then

$$v_l(t) = V_L \sin(\omega_l t - \gamma) \tag{7}$$

$$i_l(t) = I_L \sin(\omega t - \gamma - \theta_l) \tag{8}$$

Power drawn from the load becomes

$$\begin{aligned} p_l(t) &= V_L \sin(\omega_l t - \gamma) \times I_L \sin(\omega_l t - \gamma - \theta_L) \\ &= \frac{V_l I_l \cos\theta_l}{2} - \frac{V_l I_l \cos(2\omega_l t - 2\gamma - \theta_L)}{2} \end{aligned} \tag{9}$$

If the whole process is assumed lossless, then the active component drawn at the grid side should be equal to the DC power at the load. The power difference must be recovered by the DCL capacitor or the instantaneous power of the capacitor can be written as

$$p_{\text{cap}}(t) = p_{\text{conv}}(t) - p_l(t) \tag{10}$$

The ripple power in the capacitor due to the power transfer and reactive support can be obtained as

$$\begin{aligned} p_{\text{cap}}(t) = &\left\{ \frac{-V_g I_c}{2} \cos(2\omega_g t - \theta_g) - \frac{\omega_g L_c I_c^2}{2} \sin(2\omega_g t - 2\theta_g) \right\} \\ &+ \frac{V_l I_l}{2} \cos(2\omega_l - 2\gamma - \theta_l) \end{aligned} \tag{11}$$

Through simplification, the first two terms of the above equation can be reduced as

$$p_{\text{cap}}(t) = R_g \cos(2\omega_g t + \phi) + R_l \cos(2\omega_l t - 2\gamma - \theta_l) \tag{12}$$

where R_l is the apparent power of the load and R_g is given as

$$R_g = \frac{I_c}{2}\sqrt{V_g^2 + (\omega_g L_c I_c)^2 - 2V_g\omega_g L_c I_c \sin(\theta_g)}$$
$$\phi = \tan^{-1}\left(\frac{(V_g I_c \sin(\theta_g))/2 + (\omega_g L_c I_c^2 \cos(2\theta_g))/2}{-V_g I_c \cos(\theta_g))/2 + (\omega_g L_c I_c^2 \sin(2\theta_g))/2}\right) \quad (13)$$

Equation (12) contains two oscillatory terms, caused by AC power transfer from the grid to DCL and from DCL to load side, which are twice of grid and load frequencies, respectively. Since, single-phase inverters are mostly prevalent in induction heaters (IHs), where, $f_l \gg f_g$, the resultant capacitor has high-frequency power ripples superimposed on the low-frequency ripples at 100 Hz. It is worth noting that $f_l = 0$ when DC–DC converter or three-phase DC–AC inverter is used as the cascaded converter.

This ripple power is stored in the capacitor momentarily. The total energy stored can be found by integrating the ripple power from minimum to maximum value as

$$E_{cap} = \int p_{cap}(t)\,dt \quad (14)$$

The energy transfer within the capacitor is also reflected in its voltage variation. Considering the low-frequency component of grid side that causes voltage variation from $V_{max\,g}$ to $V_{min\,g}$, and similarly the energy flowing toward the load side causes a variation of $V_{max\,l}$ to $V_{mi\,l}$ in DCL capacitor, and consequently energy stored in capacitor becomes

$$E_{cap} = \frac{1}{2}C_g\left\{V_{max\,g}^2 - V_{min\,g}^2\right\} + \frac{1}{2}C_l\left\{V_{max\,l}^2 - V_{min\,l}^2\right\} \quad (15)$$

Using $V_{DC} = (V_{max\,g,l} + V_{min\,g,l})/2$ and equating (14) with (15) results in

$$C_g V_{DC}\Delta V_g + C_l V_{DC}\Delta V_l = \frac{R_g}{\omega_g} + \frac{R_l}{\omega_l} \quad (16)$$

where $C_g = (R_g/\omega_g V_{DC}\Delta V_g)$ and $C_l = (R_l/\omega_l V_{DC}\Delta V_l)$.

The energy storage requirement is for short duration for load-side power flow, so it requires smaller capacitance. The required capacitance is dominated by the power flow that occurs at $2\omega_g$. In the worst case, the peak/min of the voltage at the DCL capacitor from both power flows would be coinciding. However, it is best to avoid the overall peak to peak from exceeding by r_v%. If the capacitance C limits the sum of these two ripples to within the allowable ripple in the DCL capacitor, then

$$C = \left(\sum_{n=g,\,l}\frac{R_n}{\omega_n}\right)\frac{1}{V_{DC}\times(r_v\%V_{DC})} \quad (17)$$

Two major observations can be drawn from the above-mentioned analysis:

- The ripple energy required for the capacitive support is higher compared with inductive support of the same amount in same scenario. The difference is due to the presence of inductor in the interface of the GSC to the grid. Equivalently, the maximum capacitive support will be less than the rated capacity of GSC.
- The ripple energy required by the power flow from the load side is dependent on apparent power of the cascaded converter and the load frequency. For induction heating application due to high load frequency, the energy storage requirement is minimal.

2.2 Control structure of the GSC

A key aspect of the proposed RPS functionality in GSC is realised by the control of the bidirectional AC–DC converter. Since the spare capacity of the converter is used for reactive support, the converter should monitor and calculate the consumed active power

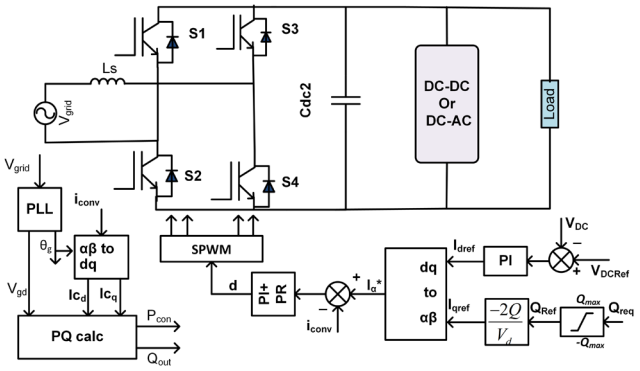

Fig. 6 *AC–DC bidirectional converter control system for RPS*

in real time. This information can be extracted by applying single-phase dq transformation to the converter output current and its orthogonal component, which serves as the signals in stationary reference frame. The required orthogonal signal for the dq transformation can be attained using transfer delay or all-pass filter or second-order generalised structure [33]. Thus, the obtained current components in the dq-axis are current components responsible for active and reactive powers provided rotating frame is properly synchronised with the grid voltage. The required synchronisation signal for transformation can be obtained from single-phase phase-locked loop [34]

$$\begin{bmatrix} i_d \\ i_q \end{bmatrix} = \begin{bmatrix} \sin\theta_g & -\cos\theta_g \\ \cos\theta_g & \sin\theta_g \end{bmatrix}\begin{bmatrix} i_\alpha \\ i_\beta \end{bmatrix} \quad (18)$$

From the active (d) and reactive (q) current components, the active (P) and reactive power (Q) can be calculated and vice versa

$$I_d = \frac{2P}{V_d}$$
$$I_q = \frac{-2Q}{V_d} \quad (19)$$

where V_d is the active component of the grid voltage or the magnitude, and it is assumed that V_q is zero for transformation synchronised with the grid voltage. A simpler modification is sufficient to generate an additional reactive power component, which is equivalent to varying the phase difference of the converter current for grid voltage. Fig. 6 illustrates the general block diagram of the control system for the home appliance. The cascaded converter only operates during active power consumption, which is determined by the load. The control system for bidirectional AC–DC is a dual-loop control structure. The external control loop maintains the DCL capacitor to a specified reference value by drawing an active power component (I_d) from the grid, thereby regulating real power flow. The reference reactive current component (I_q) is determined based on the required reactive support from the home appliance. These two serve as the reference current components in the rotating dq-frame, which are then converted to the stationary reference frame and served as a reference current for inner current control loop. The current control loop is responsible to ensure the converter output current follows the reference current accurately. The inverse dq transformation follows the equation given in (18) and only α component is used

$$I_{ref}^* = I_d^*\sin\theta_g + I_q^*\cos\theta_g \quad (20)$$

It is imperative to ensure that the reference current does not exceed the converter capacity. Hence, a limiter is added before the reactive current component reference

$$Q_{ref} = \min(Q_{free}, Q_{req}) \quad (21)$$

where the maximum possible reactive capability available at that instant from the appliance consuming an active power of P_{con} is calculated as

$$|Q_{free}(t)| \leq \sqrt{S^2 - P_{con}(t)^2} \tag{22}$$

This is computed periodically based on the real power consumption, which also includes a portion of active power to deal with the losses in the appliance converter.

A simulation of the GSC rated at 2000 VA is performed to illustrate the working of the suggested control approach. Fig. 7 shows the active, reactive and apparent power profile of the GSC as the power drawn by load and reactive reference changes. The apparent power remains constant, except at the transitory phase where the power exceeds the rated value momentarily. This can be reduced by using a limiter in the reference current to the inner current control loop and optimising the outer voltage control. This figure also shows the active power priority of the appliance with reactive reference going to zero when the power supply is fully utilised at $t = 10$ s. At another instance, the reactive reference is limited by the available maximum reactive capability, which, in turn, is calculated using the active power consumed by the load. Furthermore, a zoomed-up grid voltage, and converter output current is shown to depict the switching of the converter from inductive support mode to capacitive support mode at $t = 0.4$ s.

2.3 GSC power losses

Practically, a small portion of active power is wasted in the converter itself to offset the losses in switches and in parasitic components which is given as

$$P_{loss} = P_{cond} + P_{swt} \tag{23}$$

The switching operation (turning ON and OFF) results in switching loss P_{swt}, which is obtained by time integrating switch current and reverse voltage across the switch. This is calculated for both instants turning ON and turning OFF of switch

$$P_{swt} = \frac{1}{2} V_{DC} I_{avg} f_{sw} (t_{on} + t_{off}) \tag{24}$$

where I_{avg} is the average converter current given as $I_{avg} = (2I_C/\pi)$ and t_{on}, t_{off} are switches turn ON and turn OFF durations. Metal–oxide–semiconductor field-effect transistor (MOSFET) is the most popular switching device for high switching frequencies AC–DC converters. Similarly, the conduction losses on switches (due to turn ON resistance and turn ON voltage) and parasitic components are given as

$$P_{cond} = (V_{son} \times I_{cr}) + r_s I_{cr}^2 + r_p I_{cr}^2 \tag{25}$$

where V_{son} is the switch turn ON voltage and r_s and r_p are the switch turn ON and lumped parasitic resistance of the GSC, respectively. With additional reactive current component, the converter loss is also affected, albeit a little. The peak/root-mean-square (RMS) current can be written in terms of active and reactive current components as

$$\begin{aligned} I_C &= \sqrt{2} I_{cr} = \sqrt{I_d^2 + I_q^2} \\ I_d &= I_C \cos\phi \\ I_q &= I_C \sin\phi \end{aligned} \tag{26}$$

The range of power factor of an appliance in operation depends on amount of support extended by appliance in A2G operation mode.

3 Proposed smart home RPS system

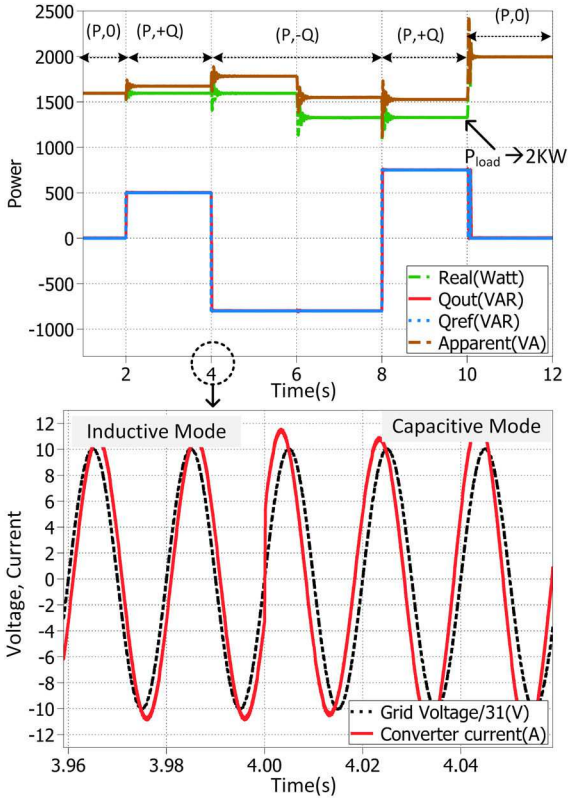

Fig. 7 *Active and reactive power profiles of single GSC*

3.1 Home energy management system

The residential homes may contain energy sources such as a utility, PV system and battery. There are a wide range of electrical loads for residential applications such as lighting, induction heating, air conditioner (AC), refrigerator, WM, television, vacuum cleaner etc. The presence of HEMS and smart meters are transforming homes into smart homes. These supervisory units control and coordinate the energy generation, usage and storage [24, 35]. The HEMS constitutes of a home server and an energy management and communication unit (EMCU). EMCU located at each outlet with the appliance has three major functions: (i) measuring the appliances' energy usage, voltage and current signals through sensors, (ii) transferring the collected data to the home server and receiving signals from the home server and (iii) managing the power supply to the appliances.

The EMCU communicates with the home server via a home area network implemented either with wireless (e.g. ZigBee, wireless fidelity etc.) or wired (i.e. power line communication) technologies [36, 37]. A home server aggregates and processes the measured information such as power consumption and status profile of appliances and lights. It also has a database, where it can store crucial current and historical information about energy consumption of appliances, their operation times etc. Through appropriate programming, the data can be analysed to extract information regarding their utilisation times and usage pattern. For instance, using the historical usage pattern (P_{con}) of home appliance, its reactive reserve potential can be estimated. The home server can also feedback the control signals dynamically to the home appliances to regulate its operation through power control subunit in the EMCU.

3.2 Proposed structure for RPS

Fig. 8 illustrates the overall structure of the proposed architecture, which is a three-level hierarchical control system structure. At top level is centralised controller operated by utility, which calculates the reactive reference at different locations and coordinates with home servers under its jurisdiction. The home server acts as supervisory controller, where additional algorithms for calculating and allocating reactive support to each appliance are executed. At

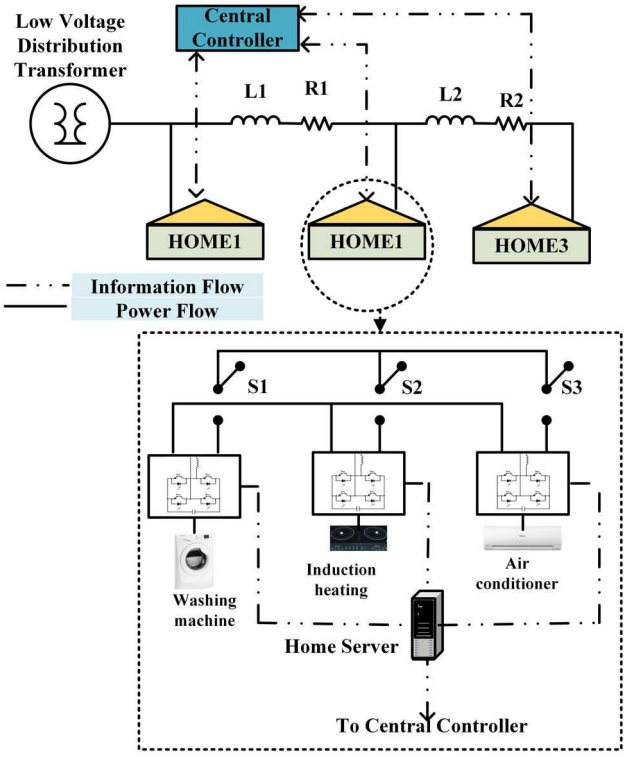

Fig. 8 *General architecture of the smart home*

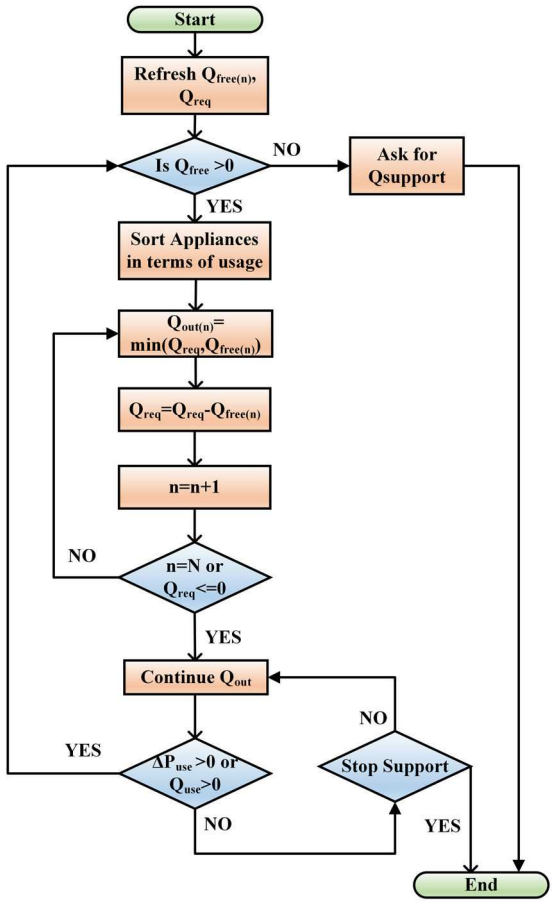

Fig. 9 *Control algorithm for allocation of reactive support to candidate appliances*

the lowest level, it is the controller implemented in home appliances, which regulates the output power of the front-end converter. The loads besides consuming active power will support (consume or inject) the reactive power to the grid. For simplicity, we assume the home server has received the reactive power reference either from the local controller measurements or through the central controller located at the utility side. This reactive reference is a function of the voltage measurement at point of common coupling (PCC), required reactive power from the home and available reactive power capability in that period. The reference can also be dynamically adjusted by the utility operator via a communication network presented by smart grid for optimising the performance based on real-time scenario. If there is shortage of reactive support from that home, the home server notifies the central controller, which will then look for other alternatives. The home server should be able to distinguish between different available appliances and have knowledge of accessible reactive power from each while it requests for RPS from them. This is achieved through a distributor, which prioritises the home appliances for RPS operation. The high-ranked appliances are first enabled for the reactive support and the remaining reactive power if any is then requested from the second-ranked appliance and so on. The algorithm to allocate the total reactive power among the home appliances is shown in Fig. 9. The details of appliance prioritisation technique are discussed in the next section.

An outer control loop using a hysteresis control, as shown in Fig. 10, is implemented to trigger the distribution algorithm whenever the error between the reactive reference and reactive support exceeds a predefined threshold. This can occur when either the reactive reference changes or the total RPS provided. The appliance's active power consumption can reduce its reactive support capacity, which, in turn, will decrease overall reactive support generated from home. The deficit reactive support has to be allocated to other appliances which are realised by the distributor. If the reactive output is within defined range of requested reactive support, no action is taken.

3.3 Operational priority of appliances

Two categories of appliances are defined based on their possible operating modes. Type '0' can only provide either active power or RPS at a particular instant, i.e. (P_{app}, 0) or (0, Q_{supp}), while Type '1' can provide reactive support during appliance operation, i.e. including additional operation mode (P_{app}, Q_{supp}). A Type '0' appliance in operation is not considered for reactive support while a Type 1 can utilise its spare power processing capacity to support reactive power. The distributor has to derive the operational priority of the appliances for A2G mode of operation. Several factors can be taken into account: minimising number of appliances to reduce management complexity, sharing the operation times to maintain useful running period, reducing the power loss associated with the reactive support and full availability of appliances. These criteria result in different orders of the appliance's priority. For instance, to have minimum number of appliances, the appliances should be sorted based on their available reactive support capacity. While for having similar operation times of each appliance, the appliances should be sorted based on their usage times.

For optimum grading, these criteria have to be considered in appropriate weightings. For simplification, in this paper, we opt to distribute the usage time equitably among the candidate appliances. This is to ensure all appliances of GSC have proportional usage overall, combining both for primary and ancillary functions. Hence, the available appliance in the pool having least usage is considered first for the reactive support and second least used appliance is considered for remaining reactive support and so on. Moreover, if the reserve reactive capacity is below the minimum defined value, the home server will exclude it from the list of candidate appliances. The home server through EMCU can monitor and track the status, power consumption and reactive support of all the appliances. Counting the number of clock pulses during the appliance operation, the appliance usage time can also be noted. To prevent changing back and forth of appliance priority while it is being used, the priority can be updated periodically which can be defined in the home server.

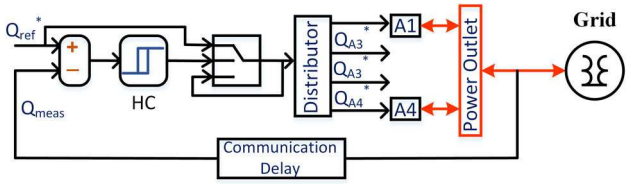

Fig. 10 *Reactive power reference control structure*

Table 2 Simulation parameters for appliances

Appliance	Power, VA	Type	Usage, h
WM	400	0	100
IH	2000	1	300
AC	1800	1	150
DW	500	0	200

Table 3 Available reactive support calculation

Usage	Type	Q_{avail}
1	0	0
1	1	Q_{spare}
0	1	Q_{spare}
0	0	Q_{spare}

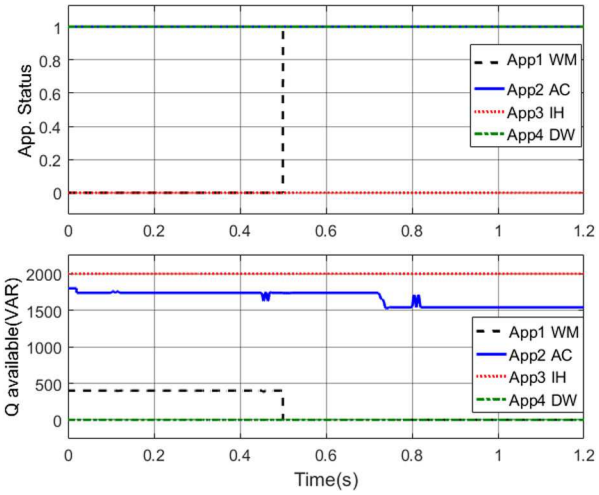

Fig. 11 *Appliance status and their reactive power capability*

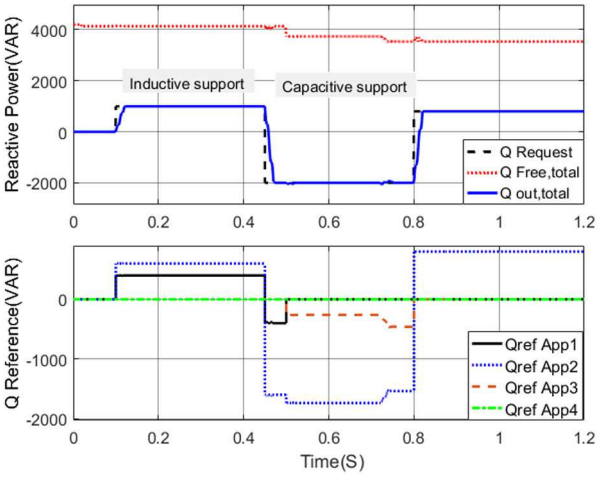

Fig. 12 *Reactive power reference allocation to appliances*

4 Simulation results

The home server algorithm in Fig. 9 for allocating reactive support to appliance is studied through simulation results. The simulation model is constructed in MATLAB/Simulink. The home is connected to a distribution grid of 240 V RMS at 50 Hz and is composed of four appliances, which can engage in grid reactive support. These participating appliances have updated topologies and control structure; hence, they are able to provide A2G mode of operation. The power converters of the appliances are assumed ideal (controlled current source) and the communication delay between appliances and home server is neglected regarding the time scale of the RPS responses. The current sensor in EMCU feedbacks the measured current information to home server, which also tracks the utilisation of the home appliances. The appliances and their corresponding parameters are given in Table 2. On the basis of the usage of the appliances, the rank of appliances for A2G support becomes in the order {WM, AC, DW, IH}. Type 0 appliance supports only two modes of operations (P, 0)*and*(0, Q), while Type 1 can support additional (P, Q) operation mode. Hence, the available reactive capability from each appliance is a function of appliance usage, spare capacity and type. The available reactive support from the appliance for different combinations is shown in Table 3. Appliance usage is considered '1' if $P_{app} > 0$ and '0' indicates the appliance is in an idle state. The required inputs for the reactive support allocation are the real-time appliance status (usage) and spare reactive capacity (Q_{spare}). The appliance is sorted in ascending order of their priority for the A2G operation. For our paper, we assume an external signal is received by the home server in the form of 'reactive request (VAR)'. This can either be for fulfilling the reactive needs of household loads (internal) or improving the voltage stability of the distribution power system in the neighbourhood (external) via RPS. Depending on the reactive power demand, the home server/supervisory control will enable or disable the home appliance power supplies to participate in the A2G operation mode.

Fig. 11 shows the appliance status and their corresponding spare reactive capability for A2G operation mode. When WM comes into operation at $t = 0.5$ s, its reactive capability drops to zero as it is fully operational and it is a Type '0' appliance. Similarly, dishwasher (DW) being in operation throughout does not have any reactive support capability at that instant even though it is being placed in the pool of candidate appliances. IH has full reactive capability while the spare power processing capacity of the AC can still be used for reactive support. In Fig. 12, the reactive request, free reactive power capability and the actual overall reactive support provided by the home is shown. The reactive reference changes at $t = 0.45$ s from inductive support to capacitive support (−2000 VAR) and again back to 1000 VAR at $t = 0.8$ s. At these instants, the home server allocates the reactive reference to the home appliances according to their priority of support. It can be seen, initially, WM and AC share the support as they are first two appliances on the list. When WM comes into operation at $t = 0.5$ s, the reactive support is then again reallocated to the appliances. Since power supply of AC alone cannot cater for the requirement, the remaining reactive support (−262 VAR) is requested from the next available appliance for reactive support, i.e. IH. At $t = 0.72$ s, the active power consumption of the AC increases which reduces its reactive capability from 1738 to 1540 VAR. Hence, the reactive support from AC is reduced to −1540 VAR while from IH is increased to −460 VAR while maintaining the total amount of reactive support being provided by the home. Fig. 13 illustrates the active power, reactive power and apparent power variations of the AC over some time ($0.7 \le t \le 1$ s). When the AC active power increases, correspondingly the spare reactive capacity; hence, the reactive output power also reduces accordingly. The appliance also switches to $P + Q$ mode from $P - Q$ mode of support at ($t = 0.8$ s), as obvious from the phase lag/lead of the converter current for the grid voltage, demonstrating its variable operation modes.

5 Cost–benefit analysis

The economic and technical benefits brought to the power network operation from the proposed method is discussed in this section. For simplification, only the operational cost while the appliance is endorsing reactive support to grid is considered while initial changeover cost and maintenance cost is ignored. The operational

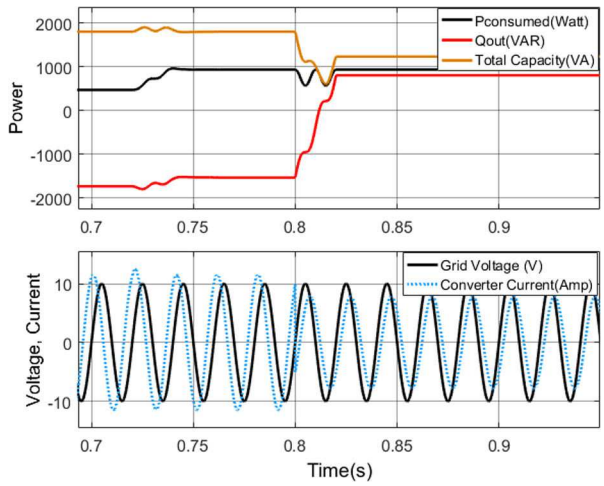

Fig. 13 *Power profile and support from the GSC of appliance A/C*

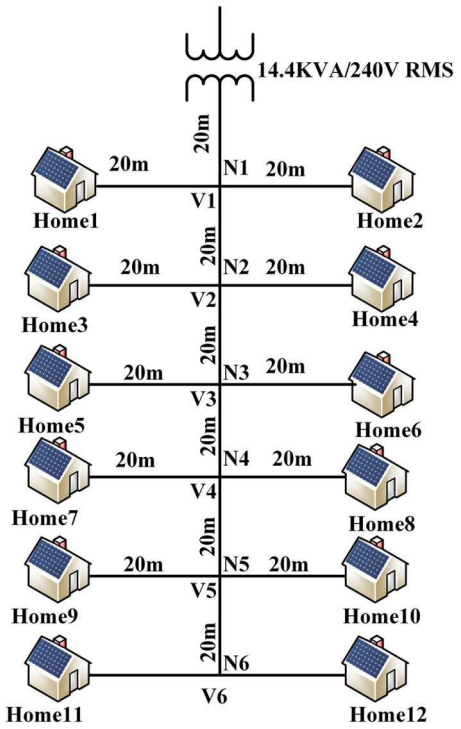

Fig. 14 *Test residential low-voltage distribution feeder*

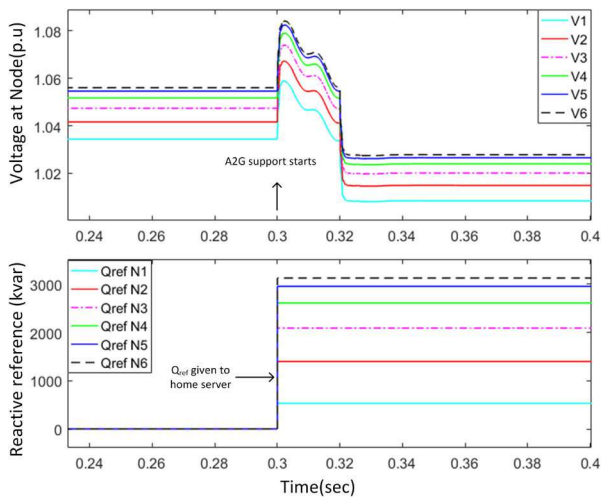

Fig. 15 *Voltage profile and reactive power references before and after application of A2G support at each node*

cost is from the additional active power losses comprising of switching and conduction loss while appliance is providing A2G operation. If CR_P is the cost of 1 kWh of consumed energy, the reactive support cost (RSC), the home appliance owner has to bear becomes

$$\text{RSC} \simeq \Delta P_{\text{loss}} \times \text{CR}_P \tag{27}$$

The monetary incentive (MI) appliance owner will be getting from the RPS at the rate of CR_Q (1 kVArh) for exchange of reactive power ΔQ_{supp} is given as

$$\text{MI} = (\Delta Q_{\text{supp}} \times \text{CR}_Q) \tag{28}$$

As real power cost is generally higher than reactive power value, the grid operator should bear the price of RSC such that MI becomes earning for the appliance owners. From the grid operator point of view, availing the service of home appliance should also bring additional economic and technical advantages in power network operation. Previous studies have already clarified that distributed reactive source realised using distributed energy resources (PV inverters) are cost-effective and reduce network losses while compared with traditional approach such as using switched capacitor [38]. The benefits are also valid for home appliances as they too provide dynamic reactive power at distribution level on receiving request signal from utility conveyed by home server.

A case study is presented here to exemplify the additional economic benefits brought to the grid operation by the proposed source of reactive power. A low-voltage residential feeder consisting of 12 houses shown in Fig. 14 is used for this study, and the parameters and system descriptions are detailed in [12]. These are also called net-zero energy solar house, where power consumption and generation are equivalent for 1 year. Each house equipped with PV rooftop system, local load and RPS qualified home appliance. Overall maximum net export of 75 kW is allowed to grid from 12 houses, while maximum reactive capability from each home for A2G operation is assumed to be 3.6 kVAr. At daytime, the grid is susceptible to overvoltage problem when PV generation peaks and local demand is lowest. Two droop control-based approaches: (i) curtailing the PV output power (APC) and (ii) using appliance for absorbing reactive power (A2G) are compared from economic point of view for addressing the overvoltage problem. In APC, active power of the PV unit is reduced linearly when local grid voltage crosses 1.03 pu until 1.06 pu, when the PV will cease to inject power to grid. Similarly for A2G, starting from 1.03 pu, the home appliance will start to absorb reactive power linearly, and at 1.06 pu full support is employed. The feeder downstream farther from the transformer is more prone to overvoltage and correspondingly sacrifice more for grid support. From simulation results, it was observed that APC technique reduced 42.35 kW of real power while A2G operation required 25.4 kVAr of reactive power consumption to restore grid voltage to nominal range at all nodes. For both cases, the required APC and A2G supports are calculated using the locally measured voltage information. The voltage profile (RMS) and reactive reference power at each node before and after application of A2G support is shown in Fig. 15. At $t = 0.3$ s, surplus RPS is provided by home appliances, thereby bringing the node voltages within admissible range while still maintaining same PV output. In A2G method, besides converter loss (0.5 kW at 98% efficiency), there is an additional loss of 3.16 kW associated with flow of reactive power in the grid's conductor referred here as network loss. Considering the peak generation occurs 2 h/day, the associated cost with each of the approach for 1 week is shown in Fig. 16. The charges for reactive power and PV power feed-in tariff are taken as AUD 0.00256/kVArh and AUD 0.0542/kWh, respectively [39]. The overall cost of applying APC is higher as compared with A2G approach as observed from cost distribution graph. However, the key concern is sharing of the monetary benefit between grid operator and the consumer such that it is a win–win situation for both. If utility is paying the price of APC, requesting A2G support

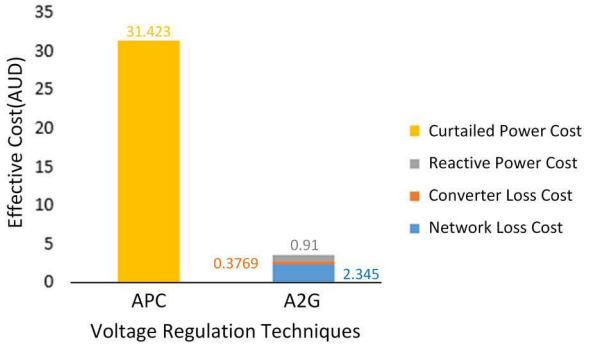

Fig. 16 *Weekly cost associated with two methods of voltage regulation*

Table 4 Example table

Parameters	Value
input voltage (V_{in})	V_{min}–$V_{max}(210-260)$ at 50 Hz
switching frequency (Hz)	50 K
output power (P_o)	1000 W
output voltage (V_{dc})	400 V
ripple current (Δi_l)	15% of I_{nom}
output voltage ripple (Δi_l)	5% of V_o

Table 5 Cost difference for 1 kW rated power supply

Component	DBR and PFC	PWM rectifier	Cost difference (element 14)
DBR	4.28 A(I_{avg})	—	−$1.892
Schottky diode	2.5 A (Av)	—	−$3.586
MOSFET	1.22 A(RMS), 6.73 A(Pk)	6.73 A(Pk)	+$36.688
MOSFET driver	1 (qty)	2 (qty)	+$4.114
inductor	1.514 mH	1 mH	NA
capacitor	397 µF	400 µF	≃ 0

and paying for cost associated with it would be economical. Contrarily, if utility prevents PV owners to inject active power for voltage regulation without any lost opportunity cost, PV owners can parallelly use A2G to improve the system's real power absorption capacity. Thereby, the real power can be injected into the grid and minimise the financial loss for PV owners.

6 Considerations for implementation

6.1 Cost increment for single power supply

The cost alteration occurred due to switch in the topological structure of the home appliance power supplies. Currently, the boost PFC in continuous conduction mode is generally preferred for the medium-power range of applications, while for high power interleaved boost PFC can be used. To evaluate the change in manufacturing cost, the difference in the cost associated with the use of components in these two different topologies can be evaluated. The selection of the components for both topologies is based on the same power rating and operational characteristics as given in Table 4. The selection of components for boost PFC is carried out using the design guidelines presented in [40]. Similarly, the selection of the switching components and inductor follows the discussion in Section 2. The switches and diodes for both topologies need to sustain voltage stress of 400 V when reverse biased, and the peak current through the switches and diode is also the same. The cost comparison for these two topological structures along with their component selections is presented in Table 5 with common components selected from same manufacturer. Although the proposed topology has higher initial component cost (AUD 18.7), it provides higher efficiency, better power quality performance and more controllability. For higher-power rated appliances such as AC and IH either interleaved boost PFC is used or bridgeless boost rectifier is used. These topologies have minimum two active switches; hence, the cost difference further goes down. This incremental cost upfront while migrating to new topology can be substantially reduced if the manufactures opt for mass production of power supplies.

6.2 Reliability of the power components

Power semiconductors (MOSFETs and insulated gate bipolar transistors) and the electrolytic capacitors are considered the most sensitive components in reliability determination of the rectifier [41]. With extended operation time or operating at full capacity, it will increase stress on power components and so will have an impact on their life. The lifetime of these devices depends on the operating scenario, time, duration and temperature. Deploying the power supplies for additional task such as A2G operation will reduce its useful life for its primary function and make it prone to failure. Equivalently, the converter may move into the wear-out period quickly. There are various reliability models of electronic elements, which can be used to dynamically calculate the reliability based on operating condition and operation times. This factor can then be accounted while distributing the reactive support to the appliances through the supervisory controller. Besides, several approaches such as active thermal management, prognosis of failures and fault-tolerant design are in place for future converter design and operation, which can assist in improving converter reliability, especially when they are supposed to be used extensively. Apart from this, the calculation of the incentive, i.e. RSC should also consider the cost of lifetime reduction of the appliance for their role in power system stability and quality. This would then encourage the customers to use their appliances for A2G support.

6.3 Billing of converter power losses

In a practical scenario, the converter is not lossless, and there occur switching and conduction losses within it during its operation. Although enforcing soft switching can reduce switching loss considerably, and efficiencies (η) of converters are getting higher through optimal design a small amount of energy is still wasted

$$p_l(t) = (1-\eta)s(t) \tag{29}$$

Even small in amount, this energy is also billed by the utility, and the customer will be charged additional amount proportional to power loss times the time of support. The additional real power further differs on the operation mode of the appliance. Again, a proper incentive proportional to the amount of RPS should be provided to the home from the utility side.

6.4 Policy modification

Electrical appliances drawing power >75 W must employ PFC as per IEC61000-3-2 [21]. Providing reactive support at the time of real power consumption equivalently implies the device to operate at some leading or lagging VAR. Moreover, RPS at distribution level from end-user appliances is yet to be accorded. This calls for introduction of standards and regulatory requirements for introducing electrical home appliances as potential reactive source/sink for grid support. Some countries such as Japan and Germany have updated grid codes to allow PV inverters at low-voltage distribution system to participate in voltage regulation by controlling active and reactive powers [7]. Similar practise can also follow for other devices at residential level, which can render RPS. The customer will have capability to provide services to the grid operators and, in turn, will be provided MIs for the same.

6.5 Secure communication network

Communication systems form the fundamental infrastructure in smart grid and smart homes. They provide a medium for transferring monitored information and control signals for facilitating power transfer. The performance of the proposed RPS from home appliance also heavily depends on the real-time transfer

of collected data such as power consumption, spare reactive capability, appliance status and so on. Hence, a reliable, minimal delay and secure communication network are imperative. Strong cyber security measures should be in place to prevent potential damages that can occur due to cyber attacks. The authenticity of the messages is key because any manipulation of the control commands by malicious attacks can cause disaster in system operation. For instance, if unintended reactive power is drawn by thousands of converters in a network, this will cause voltage degradation and may lead to voltage collapse. Also, message from home server should reach the appliances in timely fashion, since the requested reactive support may not be appropriate at other time and can cause unintentional effect. Hence, communication network should have authentication, access control and data integrity to eliminate risks of cyber attacks and improve reliability. All of these services are going to integrate into cyber infrastructure of smart grid in near future [42].

6.6 Coordination among available reactive source

In the future smart grid, it is expected that the RPS can be sourced from not only home appliances (HAs), but also various grid-interconnected systems such as PV, energy storage, EV etc. They show various features, potentials and characteristics, but the optimal integration can be more effective in providing grid support through the supervisory controller implemented in the home server. These devices have random usage behaviour, but more or less a deterministic nature. For instance, at daytime, PV inverter shows intermittency in reactive potential, EVs are generally mobile at this time, while HAs are stationary and considerable reactive capacity can be available. Contrarily at night-time, PV systems present full capacity while EVs and HAs tend to be mostly used. Through proper coordination among them, they can collectively act in mitigating voltage violations in the distribution network. However, for this, the optimum operating point of each device needs to be set through home server depending on their capacity, potential usage, load demand, priority and network condition.

7 Conclusions

The power supplies of home appliances can be mobilised for grid support through minor modification in the topology and control. This can result in a large number of distributed reactive resources in the distribution power system located closer to the reactive power requirement area. This paper presented a framework and feasibility study on how to realise the proposed A2G support. The required size of DCL capacitor for accommodating RPS is determined. An HEMS architecture supporting home appliances for RPS is presented. The control structure for selection and RPS allocation to appliance is proposed. A cost–benefit analysis of the proposed solution with APC method reflected the technical and economic benefits attainable through A2G approach. The simulation results were presented that verified the working of the proposed reactive power control structure.

8 References

[1] Thomson, M., Infield, D.: 'Impact of widespread photovoltaics generation on distribution systems', *IET Renew. Power Gener.*, 2007, **1**, (1), pp. 33–40

[2] Chaudhary, P., Rizwan, M.: 'Voltage regulation mitigation techniques in distribution system with high PV penetration: a review', *Renew. Sustain. Energy Rev.*, 2018, **82**, pp. 3279–3287

[3] Tonkoski, R., Turcotte, D., El-Fouly, T.H.: 'Impact of high PV penetration on voltage profiles in residential neighborhoods', *IEEE Trans. Sustain. Energy*, 2012, **3**, (3), pp. 518–527

[4] Olivier, F., Aristidou, P., Ernst, D., *et al.*: 'Active management of low-voltage networks for mitigating overvoltages due to photovoltaic units', *IEEE Trans. Smart Grid*, 2015, **7**, (2), pp. 926–936

[5] Xu, T., Taylor, P.: 'Voltage control techniques for electrical distribution networks including distributed generation', *IFAC Proc. Vol.*, 2008, **41**, (2), pp. 11967–11971

[6] Gautam, S., Lu, D.D.-C., Xiao, W., *et al.*: 'Feasibility study on using electrical home appliances for distributed reactive power support'. 2018 IEEE 27th Int. Symp. Industrial Electronics (ISIE), Cairns, Australia, 2018, pp. 48–54

[7] Braun, M., Stetz, T., Bründlinger, R., *et al.*: 'Is the distribution grid ready to accept large-scale photovoltaic deployment? State of the art, progress, and future prospects', *Prog. Photovolt., Res. Appl.*, 2012, **20**, (6), pp. 681–697

[8] Jahangiri, P., Aliprantis, D.C.: 'Distributed volt/VAr control by PV inverters', *IEEE Trans. Power Syst.*, 2013, **28**, (3), pp. 3429–3439

[9] Demirok, E., Sera, D., Teodorescu, R., *et al.*: 'Evaluation of the voltage support strategies for the low voltage grid connected PV generators'. 2010 IEEE Energy Conversion Congress and Exposition, Atlanta, USA, 2010, pp. 710–717

[10] Turitsyn, K., Sulc, P., Backhaus, S., *et al.*: 'Options for control of reactive power by distributed photovoltaic generators', *Proc. IEEE*, 2011, **99**, (6), pp. 1063–1073

[11] Ghasemi, M.A., Parniani, M.: 'Prevention of distribution network overvoltage by adaptive droop-based active and reactive power control of PV systems', *Electr. Power Syst. Res.*, 2016, **133**, pp. 313–327

[12] Tonkoski, R., Lopes, L.A., El-Fouly, T.H.: 'Coordinated active power curtailment of grid connected PV inverters for overvoltage prevention', *IEEE Trans. Sustain. Energy*, 2011, **2**, (2), pp. 139–147

[13] Ghosh, S., Rahman, S., Pipattanasomporn, M.: 'Distribution voltage regulation through active power curtailment with PV inverters and solar generation forecasts', *IEEE Trans. Sustain. Energy*, 2016, **8**, (1), pp. 13–22

[14] Falahi, M., Chou, H.-M., Ehsani, M., *et al.*: 'Potential power quality benefits of electric vehicles', *IEEE Trans. Sustain. Energy*, 2013, **4**, (4), pp. 1016–1023

[15] Ali, S., Pearsall, N., Putrus, G.: 'Impact of high penetration level of grid-connected photovoltaic systems on the UK low voltage distribution network'. Proc. 26th EU PVSEC, Hamburg, Germany, 2011

[16] Abad, M.S.S., Ma, J., Zhang, D., *et al.*: 'Probabilistic assessment of hosting capacity in radial distribution systems', *IEEE Trans. Sustain. Energy*, 2018, **9**, (4), pp. 1935–1947

[17] Albadi, M.H., El-Saadany, E.F.: 'A summary of demand response in electricity markets', *Electr. Power Syst. Res.*, 2008, **78**, (11), pp. 1989–1996

[18] Singh, S., Singh, B.: 'A power factor corrected PMBLDCM drive for air-conditioner using bridge converter'. 2010 IEEE Power and Energy Society General Meeting, Providence, USA, 2010, pp. 1–6

[19] Kawaguchi, Y., Hiraki, E., Tanaka, T., *et al.*: 'Feasible evaluation of a full-bridge inverter for induction heating cooking appliances with discontinuous current mode PFC control'. Power Electronics Specialists Conf. 2008 PESC 2008, Rhodes, Greece, 2008, pp. 2948–2953

[20] Pietta, L.P., Treter, M.E., Barin, J.S., *et al.*: 'Modelling and control of a high-frequency magnetron power supply for microwave heating applications'. 2015 IEEE 13th Brazilian Power Electronics Conf. First Southern Power Electronics Conf. (COBEP/SPEC), Fortaleza, Brazil, 2015, pp. 1–6

[21] Figueiredo, J.P.M., Tofoli, F.L., Silva, B.L.A.: 'A review of single-phase PFC topologies based on the boost converter'. 2010 Ninth IEEE/IAS Int. Conf. Industry Applications (INDUSCON), Sao Paolo, Brazil, 2010, pp. 1–6

[22] Park, S.M., Park, S.-Y.: 'Versatile control of unidirectional AC–DC boost converters for power quality mitigation', *IEEE Trans. Power Electron.*, 2015, **30**, (9), pp. 4738–4749

[23] Farhangi, H.: 'The path of the smart grid', *IEEE Power Energy Mag.*, 2010, **8**, (1), pp. 18–28

[24] Collotta, M., Pau, G.: 'A novel energy management approach for smart homes using Bluetooth low energy', *IEEE J. Sel. Areas Commun.*, 2015, **33**, (12), pp. 2988–2996

[25] Wilkenfeld, G.: 'Smart appliance for smart grids: flexibility in the face of uncertainty'. Proc. of ECEEE Summer Studies, 2011

[26] Yang, B., Lee, F.C., Zhang, A., *et al.*: 'LLC resonant converter for front-end DC/DC conversion'. 17th Annual IEEE Applied Power Electronics Conf. Exposition 2002 APEC 2002, Dallas, USA, 2002, vol. **2**, pp. 1108–1112

[27] Sathyan, A., Milivojevic, N., Lee, Y.-J., *et al.*: 'An FPGA-based novel digital PWM control scheme for BLDC motor drives', *IEEE Trans. Ind. Electron.*, 2009, **56**, (8), pp. 3040–3049

[28] Pandey, R., Singh, B.: 'Improved power quality SEPIC converter fed series resonant inverter for induction heater'. IEEE Int. Conf. Power Electronics, Intelligent Control and Energy Systems (ICPEICES), Delhi, India, 2016, pp. 1–6

[29] Meng, L., Cheng, K.W.E., Chan, K.W.: 'Systematic approach to high-power and energy-efficient industrial induction cooker system: circuit design, control strategy, and prototype evaluation', *IEEE Trans. Power Electron.*, 2011, **26**, (12), pp. 3754–3765

[30] Song, B.-M., Kye, M.-H., Kim, R.-Y.: 'Design of a cost-effective DC–DC converter with high power density for magnetron power supplies'. 2010 Int. Power Electronics Conf. (IPEC), Sapporo, Japan, 2010, pp. 137–141

[31] Yang, Y.-R.: 'A magnetron driver with half-bridge LLC resonant converter for microwave oven'. 2014 IEEE 23rd Int. Symp. Industrial Electronics (ISIE), Istanbul, Turkey, 2014, pp. 347–352

[32] Gautam, S., Yunqing, P., Kashif, M., *et al.*: 'DC side voltage control consideration for single phase shunt active power filter for harmonic and reactive power compensation', *J. Electr. Eng.*, 2015, **15**, (4), pp. 290–297

[33] Gautam, S., Lu, D.D.-C., Lu, Y., *et al.*: 'Fast identification of active and reactive current component for single phase grid interconnection'. 2017 20th Int. Conf. Electrical Machines and Systems (ICEMS), Sydney, Australia, 2017, pp. 1–6

[34] Golestan, S., Guerrero, J.M., Vasquez, J.C.: 'Single-phase PLLs: a review of recent advances', *IEEE Trans. Power Electron.*, 2017, **32**, (12), pp. 9013–9030

[35] Han, J., Choi, C.-S., Park, W.-K., *et al.*: 'Smart home energy management system including renewable energy based on ZigBee and PLC', *IEEE Trans. Consum. Electron.*, 2014, **60**, (2), pp. 198–202

[36] Chen, H.-C., Chang, L.-Y.: 'Design and implementation of a ZigBee-based wireless automatic meter reading system', *Prz. Elektrotech. Electr. Rev.*, 2012, **88**, (1b), pp. 64–68

[37] Yu, F.R., Zhang, P., Xiao, W., *et al.*: 'Communication systems for grid integration of renewable energy resources', *IEEE Netw.*, 2011, **25**, (5), pp. 22–29

[38] Gandhi, O., Rodríguez-Gallegos, C.D., Zhang, W., *et al.*: 'Economic and technical analysis of reactive power provision from distributed energy resources in microgrids', *Appl. Energy*, 2018, **210**, pp. 827–841
[39] Lourenço, L., Monaro, R., Salles, M., *et al.*: 'Evaluation of the reactive power support capability and associated technical costs of photovoltaic farms operation', *Energies*, 2018, **11**, (6), p. 1567
[40] Abdel-Rahman, S., Stückler, F., Siu, K.: '*PFC boost converter design guide*' (Infineon Technologies AG, Munich, 2016)
[41] Song, Y., Wang, B.: 'Survey on reliability of power electronic systems', *IEEE Trans. Power Electron.*, 2013, **28**, (1), pp. 591–604
[42] Sridhar, S., Hahn, A., Govindarasu, M., *et al.*: 'Cyber-physical system security for the electric power grid', *Proc. IEEE*, 2012, **100**, (1), pp. 210–224